

Synthesis and characterization of bis(guanidinate)lanthanide diisopropylamido complexes

New highly active initiators for the polymerizations of ϵ -caprolactone and methyl methacrylate

Yingming Yao^a, Yunjie Luo^{a,b}, Jinglei Chen^a, Zhenqin Zhang^a, Yong Zhang^a,
Qi Shen^{a,c,*}

^a Department of Chemistry and Chemical Engineering, Suzhou University, 1 Shizi Street, Suzhou 215006, China

^b Department of Biological and Pharmaceutical Engineering, Ningbo Institute of Technology, Zhejiang University, Ningbo 315104, China

^c State Key Laboratory of Organometallic Chemistry, Shanghai Institute of Organic Chemistry, Shanghai 200032, China

Received 30 April 2003; received in revised form 14 June 2003; accepted 24 June 2003

Abstract

Treatment of LnCl_3 with $[(\text{SiMe}_3)_2\text{NC}(\text{N}i\text{Pr})_2]\text{Li}$ in 1:2 molar ratio afforded the soluble bis(guanidinate)lanthanide chlorides $\{[(\text{SiMe}_3)_2\text{NC}(\text{N}i\text{Pr})_2]\text{Ln}(\mu\text{-Cl})_2\}_2$ ($\text{Ln} = \text{Y}$ (**1**), Nd (**2**)). Amination of **1** and **2** with two equivalents of $\text{LiN}(i\text{Pr})_2$ in a mixture solution of toluene and hexane gave $[(\text{SiMe}_3)_2\text{NC}(\text{N}i\text{Pr})_2]_2\text{LnN}(i\text{Pr})_2$ ($\text{Ln} = \text{Y}$ (**3**), Nd (**4**)) in good isolated yields. The single-crystal structural analyses of **2** and **3** revealed that the coordination geometries of lanthanide metals are best described as a distorted pseudo-octahedron and a pseudo-pyramid, respectively. Complexes **3** and **4** exhibited extremely high activity for the polymerizations of ϵ -caprolactone and methyl methacrylate (MMA).

© 2003 Elsevier B.V. All rights reserved.

Keywords: Organolanthanides; Guanidinate ligand; Crystal structures; Polymerization; ϵ -Caprolactone; Methyl methacrylate

1. Introduction

Over the past few decades, the most successful ancillary ligands in organolanthanide chemistry have been the derivatives of cyclopentadienyl anions [1], since lanthanocene complexes have shown highly efficient catalytic activity for a variety of olefin transformations including hydrogenation [2,3], polymerization [4], hydroamination [3,5], hydrosilylation [6] and hydroboration [7]. Recently, alternative ligand environments other than cyclopentadienyl, such as amidinates [8], guanidinate [9], β -diketiminates [10], etc. have been developed to understand their organometallic chemistry of lanthanide elements. Some of such complexes have been found

to show the exciting reactivity. For example, Arnold and co-workers [9d] reported that guanidinate aryloxides are able to initiate D,L-lactide polymerization; Piers and co-workers [11] found β -diketiminato scandium methyl complex is an effective precatalyst for ethylene polymerization; we have found that homoleptic amidinate lanthanide complexes are effective initiators for ϵ -caprolactone polymerization [8a], and guanidinate methyl lanthanide complexes show not only much higher activity than that of corresponding lanthanocene methyl complexes in the ϵ -caprolactone polymerization [9e], but also high activity in styrene polymerization [9f], which is quite difficult to achieve with the corresponding lanthanocene complexes.

In order to investigate further the effect of guanidinate ligands on the catalytic activity of the resulting lanthanide complexes, we synthesized bis(guanidinate)lanthanide diisopropylamido complexes and tested their catalytic activity for the polymerizations of

* Corresponding author. Present address: Department of Chemistry and Chemical Engineering, Suzhou University, 1 Shizi Street, Suzhou 215006, China. Tel.: +86-512-6511-2513; fax: +86-512-6511-2371.

E-mail address: qshen@suda.edu.cn (Q. Shen).

ϵ -caprolactone and methyl methacrylate (MMA). It was found that the activity of bis(guanidinate)lanthanide diisopropylamido complexes for the polymerizations of ϵ -caprolactone and MMA is higher than that of the corresponding lanthanide methyl complexes [9e]. Furthermore, to the best of our knowledge, it is the first example with respect to the catalytic activity of guanidinate lanthanide amide complexes. Here we report these results.

2. Results and discussion

2.1. Synthesis and characterization of the complexes 1–4

Treatment of a hexane solution of $[(\text{SiMe}_3)_2\text{NC}(\text{N}i\text{Pr})_2]\text{Li}$ with a diethyl ether (Et_2O) slurry of YCl_3 in 2:1 molar ratio at room temperature, after workup, afforded the neutral dimeric bis(guanidinate)yttrium chloride $\{[(\text{SiMe}_3)_2\text{NC}(\text{N}i\text{Pr})_2]\text{Y}(\mu\text{-Cl})\}_2$ (**1**) in 68% yield, as reported by Richeson and co-workers [9c]. Similar reaction of $[(\text{SiMe}_3)_2\text{NC}(\text{N}i\text{Pr})_2]\text{Li}$ with NdCl_3 in tetrahydrofuran (THF) gave $[(\text{SiMe}_3)_2\text{NC}(\text{N}i\text{Pr})_2]_2\text{Nd}(\mu\text{-Cl})_2\text{Li}(\text{THF})_2$ [9e]. Prolonged refluxing of a toluene solution of $[(\text{SiMe}_3)_2\text{NC}(\text{N}i\text{Pr})_2]_2\text{Nd}(\mu\text{-Cl})_2\text{Li}(\text{THF})_2$ led to remove the coordinated LiCl and gave neutral $\{[(\text{SiMe}_3)_2\text{NC}(\text{N}i\text{Pr})_2]\text{Nd}(\mu\text{-Cl})\}_2$ (**2**) in 76% yield.

The formula of **2** is confirmed by elemental analyses and NMR spectra. Further, X-ray structural determination of **2** reveals it to be a dimeric complex possessing two chloro bridges as shown in Scheme 1 and Fig. 1.

Complexes **1** and **2** are useful precursors for further transformation reaction. They reacted with two equivalents of $\text{LiN}(i\text{Pr})_2$ in toluene to produce monomeric and solvent-free organolanthanide amide complexes **3** and **4** according to the elemental analysis in 81 and 78% isolated yields, respectively (Scheme 1).

All the complexes are extremely air- and moisture-sensitive, and they have good solubility in toluene, diethyl ether and THF, even in hexane.

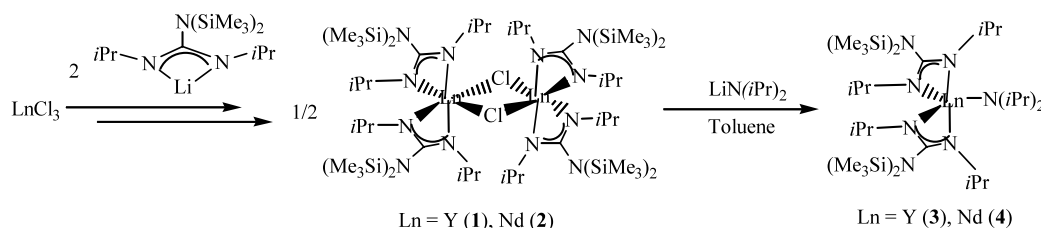
The $\text{N}=\text{C}=\text{N}$ stretch of the parent carbodiimide (2117 cm^{-1}) is absent in IR spectra of these complexes while a $\text{C}=\text{N}$ stretch at approximate 1640 cm^{-1} is observed. These data reflect that π -electrons within the double

bonds of the $\text{N}-\text{C}-\text{N}$ linkage are delocalized in all these complexes.

Crystals of **2** suitable for X-ray diffraction were grown from toluene, while **3** from DME.

An ORTEP diagram depicting the molecular structure of **2** is shown in Fig. 1. Detailed crystal and structural refinement data are listed in Table 1 and selected bond lengths and angles are given in Table 2. As shown in Fig. 1, complex **2** consists of two edge-shared distorted octahedral $[(\text{SiMe}_3)_2\text{NC}(\text{N}i\text{Pr})_2]_2\text{Nd}$ moieties, and each moiety is bonded together through two chloro bridges. Nd ion displays a distorted octahedral geometry defined by the four nitrogen atoms of the two chelating bidentate guanidinate ligands and the two chloro ligands. With nearly equal C–N distances within the chelating guanidinate ligands (see Table 2), it is clear that the π -electrons within NCN fragments are delocalized. The guanidinate ligands bind to Nd through two nitrogen atoms to yield a planar four-membered ring with bite angle ranging from $54.5(2)^\circ$ to $54.8(2)^\circ$, which are slightly smaller than those in $\{[(\text{SiMe}_3)_2\text{NC}(\text{N}i\text{Pr})_2]\text{Y}(\mu\text{-Cl})\}_2$ [9c], $[(\text{SiMe}_3)_2\text{NC}(\text{N}i\text{Pr})_2]_2\text{Yb}(\mu\text{-Cl})_2\text{Li}(\text{THF})_2$ [9e] and consistent with those in $[(\text{SiMe}_3)_2\text{NC}(\text{N}i\text{Pr})_2]_2\text{Nd}(\mu\text{-Me})_2\text{Li}(\text{TMEDA})$ [9e]. The Nd–N bond lengths vary from $2.409(7)$ to $2.488(7)$ Å, which are close to the values reported for $[(\text{SiMe}_3)_2\text{NC}(\text{N}i\text{Pr})_2]_2\text{Yb}(\mu\text{-Cl})_2\text{Li}(\text{THF})_2$ [9e], $[(\text{SiMe}_3)_2\text{NC}(\text{N}i\text{Pr})_2]_2\text{Nd}(\mu\text{-Me})_2\text{Li}(\text{TMEDA})$ [9e] and $\{[(\text{SiMe}_3)_2\text{NC}(\text{N}i\text{Pr})_2]\text{Y}(\mu\text{-Cl})\}_2$ [9c]. The bond lengths of Nd–Cl are in the range $2.781(3)$ – $2.848(2)$ Å, which are comparable with those in $\{[(\text{SiMe}_3)_2\text{NC}(\text{N}i\text{Pr})_2]\text{Y}(\mu\text{-Cl})\}_2$ [9c]. Assigning the guanidinate ligands as occupying a single coordination site defined by the central carbon of the CN_3 moieties, the angles defined by these centroids and Nd center are $123.4(2)^\circ$ and $122.6(2)^\circ$, respectively, and they are very similar to the corresponding angles in $\{[(\text{SiMe}_3)_2\text{NC}(\text{N}i\text{Pr})_2]\text{Y}(\mu\text{-Cl})\}_2$ ($123.09(15)^\circ$ and $122.17(17)^\circ$) [9c].

The orientation of $\text{N}(\text{SiMe}_3)_2$ groups relative to NCNNd plane is approximately perpendicular (the average dihedral angle formed by the planar $\text{N}(\text{SiMe}_3)_2$ function and NdNCN plane is 89.96°), which is identical to those reported for Sm [9b], Yb [9b,9e], Nd [9e] and Y [9c] complexes. This disposition prevents π -overlapping between these two moieties; furthermore, it



Scheme 1.

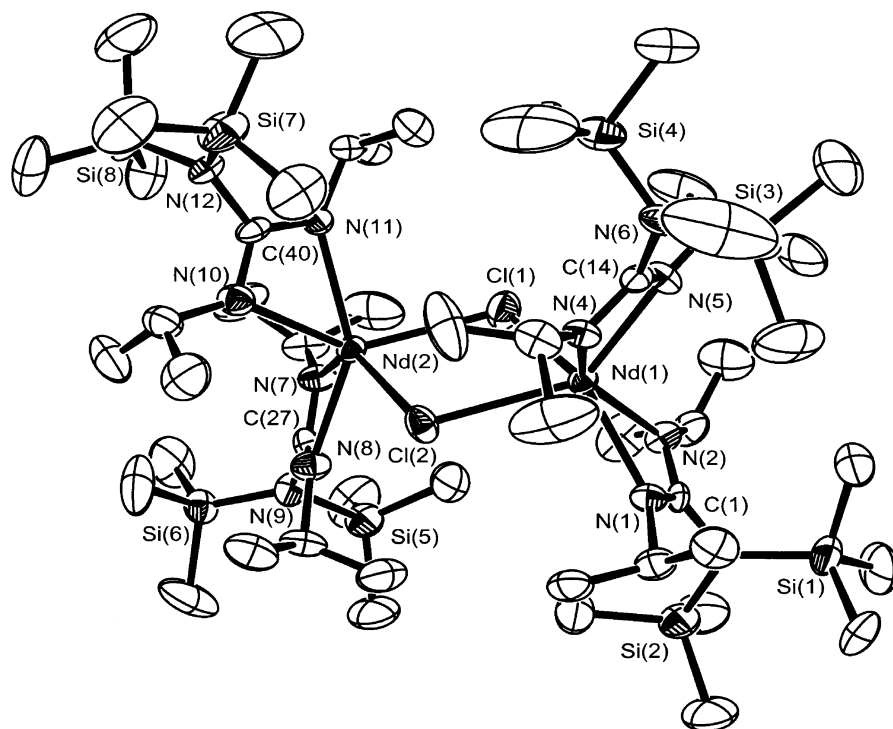


Fig. 1. ORTEP diagram of $\{[(\text{SiMe}_3)_2\text{NC}(\text{NiPr})_2]_2\text{NdCl}\}_2$ (**2**) showing non-hydrogen atom-numbering scheme.

Table 1
Details of the crystallographic data and refinements for **2** and **3**

| | 2 | 3 |
|--|---|---|
| Empirical formula | $\text{C}_{52}\text{H}_{128}\text{Cl}_2\text{Nd}_2\text{N}_{12}\text{Si}_8$ | $\text{C}_{32}\text{H}_{78}\text{N}_7\text{Si}_4\text{Y}$ |
| Formula weight | 1505.73 | 762.26 |
| Temperature (K) | 193.1 | 193.1 |
| $\lambda(\text{Mo-K}\alpha)$ (Å) | 0.7107 | 0.7107 |
| Crystal system | monoclinic | triclinic |
| Space group | $P1c1$ | $P\bar{1}$ |
| Unit cell dimensions | | |
| a (Å) | 13.2488(11) | 9.8144(2) |
| b (Å) | 14.9334(11) | 13.7802(3) |
| c (Å) | 20.954(2) | 19.52070(10) |
| α (°) | 90 | 66.35(1) |
| β (°) | 96.536(5) | 77.72(2) |
| γ (°) | 90 | 75.59(2) |
| V (Å ³) | 4118.9(6) | 2323.2(3) |
| Z | 2 | 2 |
| D_{calc} (mg m ⁻³) | 1.214 | 1.090 |
| Absorption coefficient (mm ⁻¹) | 1.463 | 1.387 |
| $F(0\ 0\ 0)$ | 1580.00 | 828.00 |
| θ range for data collection (°) | 3.1–27.5 | 3.0–27.5 |
| Reflections collected | 8839 | 10 480 |
| Independent reflections | 7794 | 6900 |
| Data/restraints/parameters | 7794/0/813 | 6900/0/475 |
| Final R indices [$I > 2\sigma(I)$] | 0.0392 | 0.0440 |
| wR | 0.1010 | 0.1000 |
| Goodness-of-fit on F^2 | 1.055 | 0.957 |

increases the steric bulk above and below the planar guanidinate ligand.

An ORTEP diagram of **3** is presented in Fig. 2. Details concerning the data collection are listed in Table 1 and selected bond lengths and angles are given in Table 3.

Complex **3** has a monomeric structure in the solid state. The geometry of Y ion can be best described as a pseudo-pyramid with the four nitrogen atoms of the two chelating bidentate guanidinate ligands forming the bottom, and the nitrogen atom of $\text{N}(\text{iPr})_2$ group defining the vertex.

The Y–N(7) bond length is 2.199(3) Å, which is consistent with La–N σ -bond lengths in $\text{La}[\text{CyNC}(\text{N}(\text{SiMe}_3)_2)\text{NCy}](\text{N}(\text{SiMe}_3)_2)_2$ (2.382(3) and 2.377(3) Å) [9d], and Er–N σ -bond length in $(\text{MeC}_5\text{H}_4)_2\text{-ErNC}_5\text{H}_{10}(\text{HNC}_5\text{H}_{10})$ (2.159(8) Å) [12], but rather shorter than those in previously characterized organo-lanthanide amides $(\text{C}_5\text{Me}_5)_2\text{YN}(\text{SiMe}_3)_2$ (2.274(5) Å) [13], $(\text{C}_5\text{Me}_5)_2\text{SmN}(\text{SiMe}_3)_2$ (2.301(3) Å) [14] and $\{\text{CyNC}[\text{N}(\text{SiMe}_3)_2]\text{NCy}\}_2\text{YbN}(\text{SiMe}_3)_2$ (2.343(19) Å) [9b], if the differences in ionic radii are considered. The bonding parameters with the two chelating guanidinate ligands are not dramatically different. Each $[(\text{SiMe}_3)_2\text{NC}(\text{NiPr})_2]\text{Y}$ moiety is a four-membered planar with N–Y–N bite angles of 56.69(9)° and 56.54(8)°, respectively. Complex **3** is an approximately C_2 symmetric molecule in which the pseudo-twofold axis lies along the Y–N(7) bond.

It can be seen in Fig. 2 that the orientation of $\text{N}(\text{SiMe}_3)_2$ groups relative to NCNY plane is also proximately perpendicular. The dihedral angle formed by C(30)N(7)C(27) plane and N(7)C(14)C(1) plane is

68.56°; this can be attributed to the steric interactions among the two guanidinate ligands and the bulky diisopropylamido group.

2.2. Polymerization of ϵ -caprolactone and MMA by complexes **3** and **4**

Complexes **3** and **4** showed high activity for the polymerization of ϵ -caprolactone under mild conditions in toluene. The preliminary results are listed in Table 4. The polymerization was completed within minutes. Even the catalyst amount decreases to 0.04 mol% ($[CL]/[I] = 2500:1$), the polymerization still gives the yield as high as 80% in the case of **4** as an initiator. The guanidinate ligand effect of the present reaction is obvious on comparison with the results reported for $(\text{MeCp})_2\text{LnN}(\text{iPr})_2(\text{THF})$ [15,16]. For example, using $(\text{MeCp})_2\text{YN}(\text{iPr})_2(\text{THF})$ as an initiator at $[CL]/[I] = 500:1$ at 20 °C for 4 h, only 88.4% of the yield of polyester was obtained [16], whilst **3** and **4** can produce the polyester in 86 and 98% yields, respectively, even at $[CL]/[I] = 2000:1$ at 15 °C in 5 min. This may be the result that the hard Lewis base of the guanidinate ligand can render the metal center more electronic-deficient. The effect of the central metals on the catalytic activity can be observed, the active order, **4** > **3**, under the present polymerization conditions is in good agreement with the increasing tendency in ionic radii ($\text{Nd} > \text{Y}$), which is similar to that found in lanthanocene complex systems [17]. The polymerization system gives the polymers with high molecular weight ($M_n > 10^4$). The higher molecular weights than theoretical values calculated by monomer to initiator ratio may be due to the low efficiency of the initiator. The molecular weight distributions are relatively broad; however, they vary little if the polymerization prolongs from 15 min to 4 h (entries 2 and 3).

It is noteworthy that under the present polymerization conditions, homoleptic guanidinate complexes $[(\text{SiMe}_3)_2\text{NC}(\text{NiPr})_2]_3\text{Ln}$ are unable to initiate the ring-opening polymerization of ϵ -caprolactone [18], which indicates the presence of $\text{Ln}-\text{N}(\text{iPr})_2$ σ -bond in $[(\text{SiMe}_3)_2\text{NC}(\text{NiPr})_2]_2\text{LnN}(\text{iPr})_2$ is crucial for the ring-opening polymerization of ϵ -caprolactone. Further spectral characterizations of the oligomer of caprolactone, prepared by the reaction of $[(\text{SiMe}_3)_2\text{NC}(\text{NiPr})_2]_2\text{YN}(\text{iPr})_2$ with ϵ -caprolactone in 1:10 molar ratio, show the presence of a terminal diisopropylamido group (see Section 4). We can envisage, at the initial stage of the polymerization, a nucleophilic attack by amidonitrogen atom at the lactone carbonyl-carbon atom followed by acyl-oxygen bond cleavage and the formation of a lanthanide alkoxide. The polymerization mechanism is illustrated in Scheme 2.

Complexes **3** and **4** can also effectively initiate the polymerization of MMA. The polymerization proceeds

Table 2
Selected bond lengths (Å) and angles (°) for **2**

| Bond length (Å) | |
|-----------------|-----------|
| Nd1–C1 | 2.885(8) |
| Nd1–C14 | 2.891(7) |
| Nd1–C11 | 2.833(2) |
| Nd1–C12 | 2.848(2) |
| Nd1–N1 | 2.409(7) |
| Nd1–N2 | 2.461(7) |
| Nd1–N4 | 2.488(7) |
| Nd1–N5 | 2.431(7) |
| Nd2–C11 | 2.781(3) |
| Nd2–C12 | 2.841(2) |
| Nd2–N7 | 2.416(7) |
| Nd2–N8 | 2.474(7) |
| Nd2–C27 | 2.907(8) |
| Nd2–C40 | 2.918(8) |
| Nd2–N10 | 2.444(8) |
| Nd2–N11 | 2.482(7) |
| N1–C1 | 1.330(11) |
| N2–C1 | 1.33(1) |
| N3–C1 | 1.449(11) |
| N4–C14 | 1.346(11) |
| N5–C14 | 1.324(11) |
| N6–C14 | 1.45(1) |
| N7–C27 | 1.330(11) |
| N8–C27 | 1.361(11) |
| N9–C27 | 1.43(1) |
| N10–C40 | 1.340(11) |
| N11–C40 | 1.349(12) |
| N12–C40 | 1.441(11) |
| Bond angles (°) | |
| C11–Nd1–C12 | 76.02(6) |
| N1–Nd1–N2 | 54.7(2) |
| N4–Nd1–N5 | 54.8(2) |
| C11–Nd2–C12 | 76.96(6) |
| N7–Nd2–N8 | 54.7(2) |
| N10–Nd2–N11 | 54.5(2) |
| Nd1–C11–Nd2 | 104.46(9) |
| Nd1–C12–Nd2 | 102.56(7) |
| Nd1–N1–C1 | 96.7(5) |
| Nd1–N2–C1 | 94.3(5) |
| Nd1–N4–C14 | 93.1(5) |
| Nd1–N5–C14 | 96.2(5) |
| Nd2–N7–C27 | 97.6(5) |
| N7–C27–N8 | 113.2(7) |
| N10–C40–N11 | 114.1(7) |
| N4–C14–N5 | 115.9(7) |
| Nd2–N11–C40 | 94.6(5) |
| Nd2–N10–C40 | 96.6(6) |
| Nd2–N8–C27 | 94.1(5) |
| Nd2–N7–C27 | 97.6(5) |
| Nd2–N10–C40 | 96.6(6) |
| Nd2–N11–C40 | 94.6(5) |
| Nd2–N8–C27 | 94.1(5) |
| N1–C1–N2 | 114.3(7) |
| C40–Nd2–C27 | 123.4(2) |
| C1–Nd1–C14 | 122.6(2) |

fluently at the temperatures below 0 °C to give PMMA with high molecular weight and rather narrow molecular weight distributions (see Table 5). The activity of the present polymerization system can be comparable with

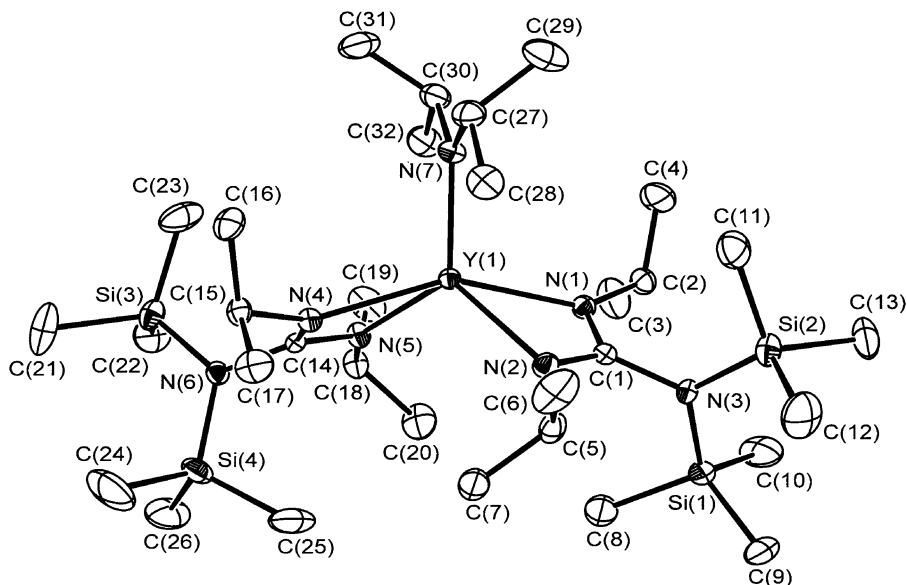


Fig. 2. ORTEP diagram of $[(\text{SiMe}_3)_2\text{NC}(\text{N}i\text{Pr})_2]_2\text{YN}(i\text{Pr})_2$ (**3**) showing atom-numbering scheme. Hydrogen atoms have been omitted for clarity.

Table 3
Selected bond lengths (Å) and angles (°) for **3**

| | |
|-----------------|-----------|
| Bond length (Å) | |
| Y1–N1 | 2.403(3) |
| Y1–N2 | 2.346(3) |
| Y1–N4 | 2.399(2) |
| Y1–N5 | 2.348(3) |
| Y1–N7 | 2.199(3) |
| Y1–C1 | 2.801(3) |
| Y1–C14 | 2.802(3) |
| N1–C1 | 1.330(4) |
| N2–C1 | 1.337(4) |
| N4–C14 | 1.324(4) |
| N5–C14 | 1.338(4) |
| Bond angles (°) | |
| N1–Y1–N2 | 56.69(9) |
| N1–Y1–N4 | 150.18(9) |
| N2–Y1–N4 | 106.61(9) |
| N1–Y1–N5 | 105.25(9) |
| N2–Y1–N5 | 115.1(1) |
| N4–Y1–N5 | 56.54(8) |
| N1–Y1–N7 | 104.77(9) |
| N2–Y1–N7 | 121.4(1) |
| N4–Y1–N7 | 105.04(9) |
| N5–Y1–N7 | 123.4(1) |
| N7–Y1–C1 | 115.5(1) |
| N7–Y1–C14 | 116.70(9) |
| C1–Y1–C14 | 127.79(9) |
| Y1–N1–C1 | 92.69(19) |
| Y1–N2–C1 | 95.04(19) |
| Y1–N4–C14 | 93.11(18) |
| Y1–N5–C14 | 95.01(18) |
| Y1–N5–C18 | 142.4(2) |
| N1–C1–N2 | 115.5(3) |
| Y1–C1–N3 | 176.8(2) |
| N4–C14–N5 | 115.3(3) |
| Y1–C14–N6 | 177.7(2) |

those of $(\text{MeC}_5\text{H}_4)_2\text{LnN}(i\text{Pr})_2(\text{THF})$ [19], $(\text{MeC}_5\text{H}_4)_2\text{-LnNC}_5\text{H}_{10}(\text{HNC}_5\text{H}_{10})$ [11] and *ansa*- $\text{Me}_2\text{Si}(\text{Ful})(\eta^5\text{-C}_5\text{H}_4)\text{LnN}(\text{SiMe}_3)_2$ [20]. The effect of the temperature on the polymerization can be observed obviously. For example, the yield decreases from 100 to 60.2% with the polymerization temperature increasing from -78 to 0 °C in the case of 200:1 molar ratio of monomer to initiator for **4**. This may be the result of higher polymerization temperature favoring the nucleophilic attack of amido group at the carbonyl-carbon atom of MMA.

The tacticity of the resultant PMMA was determined with reference to the reported triad [21]. These polymerization reactions give syndiotactic-rich PMMA (> 67%). It is interesting that the syndiotactic contents of the polymers almost have no change when the polymerization temperatures decrease from 0 to -78 °C.

3. Conclusion

In summary, we have successfully synthesized a series of new soluble bis(guanidinate)lanthanide complexes, and characterized some of their structural features by X-ray diffraction study. Moreover, we found bis(guanidinate)lanthanide diisopropylamido complexes can be served as single-component catalysts for the polymerizations of ϵ -caprolactone and MMA. The ring-opening polymerization of ϵ -caprolactone with guanidinate lanthanide amides proceeds via a coordination insertion mechanism. It is clear that the catalytic reactivity of a lanthanide complex in polymerization can be tuned by altering the ancillary ligands attached to the metal center.

Table 4
Polymerization of ϵ -caprolactone initiated by complexes **3** and **4**^a

| Entry | Initiator | [M]/[I] | Yield (%) ^b | $M_n \times 10^{-4}$ ^c | M_w/M_n ^c |
|----------------|-----------|---------|------------------------|-----------------------------------|------------------------|
| 1 | 3 | 700 | 100 | 7.99 | 2.07 |
| 2 | 3 | 1000 | 100 | 11.41 | 2.23 |
| 3 ^d | 3 | 1000 | 100 | 10.28 | 2.36 |
| 4 | 3 | 1500 | 93 | 17.12 | 1.78 |
| 5 | 3 | 2000 | 86 | 22.83 | 1.94 |
| 6 | 4 | 1000 | 100 | 11.06 | 2.15 |
| 7 | 4 | 1500 | 100 | 29.82 | 2.26 |
| 8 | 4 | 2000 | 98 | 32.29 | 1.87 |
| 9 | 4 | 2500 | 80 | 28.18 | 2.06 |

^a Polymerization conditions: in toluene; 5 min; 15 °C; solvent/monomer = 5 (v/v).

^b Yield = weight of polymer obtained/weight of monomer used.

^c Measured by GPC calibrated with standard polystyrene samples.

^d 4 h.

4. Experimental

All manipulations were performed under pure argon with rigorous exclusion of air and moisture using standard Schlenk techniques. Solvents were distilled from Na/benzophenone ketyl prior to use. Deuterated benzene (C_6D_6) was purchased from Acros, and dried over sodium and vacuum-transferred. *N,N'*-Diisopropylcarbodiimide was purchased from Aldrich and purified by distillation under reduced pressure. MMA, a commercial reagent (chemically pure) of Beijing Chemical Factory, was distilled over calcium hydride (CaH_2) and stored over molecular sieves 4 Å under argon. ϵ -Caprolactone was purchased from Acros, dried by stirring with CaH_2 for 48 h, and then distilled under reduced pressure. Anhydrous $LnCl_3$ [22], $[(SiMe_3)_2NC(NiPr)_2]Li$ [9e] and $\{[(SiMe_3)_2NC(NiPr)_2]_2Y(\mu-Cl)_2\}$ (**1**) [9c] were prepared according to the literature procedures. Melting points were determined in argon-filled capillary tubes and are uncorrected. Lanthanide metal analyses were carried out by complexometric titration. The content of lithium was determined on a Hitachi 180-80 polarized Zeeman atomic absorption spectrophotometer. Carbon, hydrogen and nitrogen analyses were performed by direct combustion on a Carlo-Erba EA-1110 instrument. IR spectra were recorded with a Nicolet Magna-IR 550

spectrometer. 1H -NMR and ^{13}C -NMR spectra were obtained using a Unity Inova-400 spectrometer. Molecular weight and molecular weight distributions were determined against polystyrene standard by gel permeation chromatography (GPC) with a Waters 1515 apparatus equipped with a set of Waters Styragel HR columns (HR-1, HR-2 and HR-4 columns, effective molecular weight range, 100–5000, 500–20 000 and 5000–500 000, respectively). THF was used as an eluent at a flow rate of 1.0 ml min⁻¹ at 30 °C.

4.1. Synthesis of $\{[(SiMe_3)_2NC(NiPr)_2]_2Nd(\mu-Cl)_2\}$ (**2**)

A hexane (50 ml) solution of $[(SiMe_3)_2NC(NiPr)_2]Li$ (6.08 g, 20.72 mmol), 2.60 g of $NdCl_3$ (10.37 mmol) and 100 ml of THF was combined in a flask. The reaction was allowed to continue at room temperature for 2 days. Then, the volatiles were removed under reduced pressure. The blue residue was dissolved in 100 ml of toluene, and then was heated at refluxing temperature for 2 h. LiCl was removed by centrifugation, and the blue supernatant was concentrated to 20 ml. Cooling to -15 °C overnight yielded blue cubic crystals of **2** (5.72 g, 7.88 mmol, 76%). m.p. 156–158 °C. Anal. Calc. for $C_{52}H_{128}Cl_2Nd_2N_{12}Si_8$: C, 41.48; H, 8.59; N, 11.17; Nd, 19.16. Found: C, 40.86; H, 8.51; N, 10.92; Nd, 19.06%.

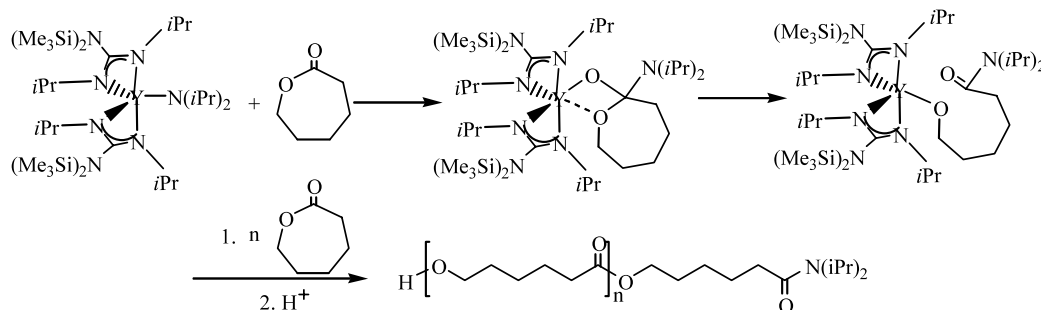


Table 5
Polymerization of MMA initiated by complexes **3** and **4**^a

| Entry | Initiator | [M]/[I] | Temperature (°C) | Yield (%) ^b | $M_n \times 10^{-4}$ ^c | M_w/M_n ^c | <i>mm</i> | <i>mr</i> | <i>rr</i> |
|-------|-----------|---------|------------------|------------------------|-----------------------------------|------------------------|-----------|-----------|-----------|
| 1 | 3 | 1000 | −78 | 96.8 | 13.22 | 1.90 | | | |
| 2 | 3 | 500 | −78 | 99.2 | 11.08 | 1.91 | 15.2 | 17.0 | 67.8 |
| 3 | 3 | 500 | 0 | 58.8 | 9.08 | 1.83 | 15.1 | 17.5 | 67.4 |
| 4 | 3 | 200 | −78 | 93.5 | 12.56 | 1.38 | | | |
| 5 | 3 | 200 | 0 | 58.3 | 9.61 | 1.85 | | | |
| 6 | 4 | 200 | −78 | 100 | 11.67 | 1.13 | | | |
| 7 | 4 | 200 | 0 | 60.2 | 3.03 | 1.68 | | | |
| 8 | 4 | 200 | 10 | 41.9 | 3.20 | 1.72 | | | |
| 9 | 4 | 500 | −78 | 100 | 9.83 | 1.63 | 6.8 | 19.1 | 74.1 |
| 10 | 4 | 500 | 0 | 46.3 | 8.33 | 1.78 | 5.2 | 23.8 | 71.0 |
| 11 | 4 | 700 | −78 | 100 | 17.11 | 1.51 | | | |

^a Polymerization conditions: in toluene; 2 h, solvent/monomer = 2 (v/v).

^b Yield = weight of polymer obtained/weight of monomer used.

^c Measured by GPC calibrated with standard polystyrene samples.

¹H-NMR (C_6D_6 , δ): 4.16, 3.85 (m, 8H, $CHMe_2$), 1.34, 1.10 (d, 48H, $CH(CH_3)_2$), 0.23, 0.16 (s, 72H, $Si(CH_3)_3$) ppm. IR (KBr pellet, cm^{-1}): 3314 (m), 2967 (s), 1640 (s), 1469 (m), 1385 (m), 1331 (w), 1307 (w), 1253 (s), 1180 (m), 1053 (s), 952 (s), 841 (s), 756 (m), 682 (m).

4.2. Synthesis of $[(SiMe_3)_2NC(NiPr)_2]_2YN(iPr)_2$ (**3**)

A Schlenk flask was charged with **1** (1.45 g, 2.08 mmol) and 50 ml of hexane. The solution was added $LiN(iPr)_2$ (0.44 g, 4.20 mmol) in 30 ml of hexane at 0 °C. The reaction mixture was kept at 0 °C for 1 h, then slowly warmed to room temperature and stirred overnight. After removal of volatiles under vacuum, the white residue was extracted with hexane and LiCl was removed by centrifugation. The supernatant was removed in vacuo and 5 ml of DME was added. Cooling to −15 °C for 2 weeks gave **3** as colorless cubic crystals. Yield, 1.28 g (1.68 mmol, 81%). m.p. 122–125 °C. Anal. Calc. for $C_{32}H_{78}N_7Si_4Y$: C, 50.42; H, 10.34; N, 12.87; Y, 11.66. Found: C, 49.32; H, 10.31; N, 12.54; Y, 11.58%. ¹H-NMR (C_6D_6 , δ): 3.92 (m, 4H, $CHMe_2$), 3.61 (m, 2H, $CHMe_2$), 1.53, 1.51 (d, 12H, $CH(CH_3)_2$), 1.34, 1.32 (d, 24H, $CH(CH_3)_2$), 0.36 (br, 36H, $Si(CH_3)_3$) ppm. ¹³C-NMR (C_6D_6 , δ): 169.52 (CN_3), 49.35, 46.97 ($CHMe_2$), 30.14, 27.86 ($(CH_3)_2CH$), 3.72 ($CN(Si(CH_3)_3)_2$) ppm. IR (KBr pellet, cm^{-1}): 3445 (w), 2967 (s), 1639 (s), 1469 (m), 1450 (m), 1362 (w), 1327 (w), 1253 (s), 1230 (m), 1180 (m), 1049 (m), 952 (s), 918 (s), 841 (s), 760 (m), 682 (m).

4.3. Synthesis of $[(SiMe_3)_2NC(NiPr)_2]_2NdN(iPr)_2$ (**4**)

As for the synthesis of **3**, using 1.29 g (0.86 mmol) of **2**, 0.18 g of $LiN(iPr)_2$ (1.72 mmol) and 50 ml of hexane. Recrystallization from hexane gave blue cubic crystals. Yield, 0.55 g (0.67 mmol, 78%). m.p. 118–120 °C. Anal.

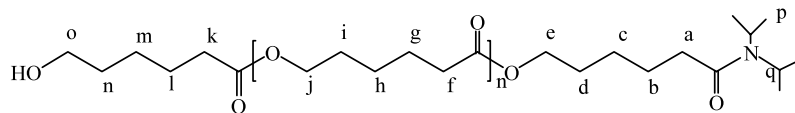
Calc. for $C_{32}H_{78}NdN_7Si_4$: C, 47.01; H, 9.64; N, 12.00; Nd, 17.64. Found: C, 46.88; H, 9.56; N, 11.93; Nd, 17.35%. ¹H-NMR (C_6D_6 , δ): 3.76 (m, 4H, $CHMe_2$), 3.03 (m, 2H, $CHMe_2$), 1.33 (d, 12H, $CH(CH_3)_2$), 1.10, 1.00 (d, 24H, $CH(CH_3)_2$), 0.23 (s, 36H, $Si(CH_3)_3$) ppm. IR (KBr pellet, cm^{-1}): 3445 (w), 2967 (s), 2870 (m), 1640 (s), 1470 (m), 1451 (m), 1377 (m), 1331 (w), 1254 (s), 1181 (m), 1053 (s), 957 (s), 918 (s), 879 (m), 841 (s), 760 (m), 683 (m).

4.4. Polymerization reactions

The procedures for the polymerization of ϵ -caprolactone and MMA by complexes **3** and **4** are the same, and a typical polymerization reaction is given below (entry 1, Table 4). A 50-ml Schlenk flask equipped with a magnetic stir bar was charged with 1 ml of ϵ -caprolactone and 3.7 ml of toluene. To this solution was added 1.3 ml of initiator (10.0 mM in toluene) via a syringe. The contents of the flask were then stirred vigorously at 15 °C for 5 min, during which time the mixture became very viscous, then disrupting the stirring. The reaction mixture was quenched by the addition of 1 M HCl solution and was then poured into ethanol to precipitate the polymer, which was dried under vacuum and weighed.

4.5. Synthesis of oligomer of caprolactone initiated by **3**

A 50-ml Schlenk flask equipped with a magnetic stir bar was charged with 9 ml of **3** (10.0 mM in toluene). To this solution was added 0.1 ml of ϵ -caprolactone via a syringe. The contents of the flask were stirred vigorously at 8 °C for 5 min, and quenched by the addition of 1 M HCl solution. Then the solution was poured into 50 ml of methanol to precipitate the white oligomer. After being washed with methanol for three times, the oligomer was collected and dried under vacuum. ¹H-



NMR (CD_3Cl , 25 °C, δ): 1.34 (m, Hh), 1.34 (m, Hm), 1.38 (m, Hc), 1.42 (m, Hn), 1.51 (m, Hp), 1.61 (m, Hd), 1.61 (m, Hg), 1.61 (m, Hi), 1.61 (m, Hl), 1.69 (m, Hb), 2.29 (t, Hf), 2.29 (t, Hk), 2.33 (t, Ha), 3.65 (br s, Ho), 3.88 (m, Hq), 4.07 (t, Hj), 4.24 (t, He) ppm. IR (KBr pellet, cm^{-1}): 3441 (w), 2948 (s), 2866 (m), 1728 (s), 1474 (m), 1420 (m), 1381 (m), 1331 (m), 1242 (s), 1188 (m), 1045 (m), 960 (m), 733 (w).

4.6. X-ray structural determination of **2** and **3**

Single crystals were sealed in a thin-walled glass capillary filled with argon for X-ray structural analysis. Diffraction data for **2** and **3** were collected on a Rigaku Mercury CCD area detector. The structures were solved by direct methods and refined by full-matrix least-squares procedures based on $|F|^2$. All non-hydrogen atoms were refined with anisotropic displacement coefficients. Hydrogen atoms were treated as idealized contributions. The structures of both **2** and **3** were solved and refined using CRYSTALS programs.

5. Supplementary material

Crystallographic data for the structural analysis have been deposited with the Cambridge Crystallographic Data Center, CCDC No. 197588 for complex **2** and No. 197589 for complex **3**. Copies of this information may be obtained free of charge from the Director, CCDC, 12 Union Road, Cambridge CB2 1EZ, UK (Fax: +44-1223-336033; e-mail: deposit@ccdc.cam.ac.uk or www: <http://www.ccdc.cam.ac.uk>).

Acknowledgements

We are grateful to the Chinese National Natural Science Foundation for financial support.

References

- [1] (a) H. Schumann, J.A. Meese-Marktscheffel, L. Esser, *Chem. Rev.* 95 (1995) 865; (b) C.J. Schaverien, *Adv. Organomet. Chem.* 36 (1994) 283; (c) H. Schumann, *Angew. Chem. Int. Ed. Engl.* 23 (1984) 474; Reviews: [2] (a) W.J. Evans, I. Bloom, W.E. Hunter, J.L. Atwood, *J. Am. Chem. Soc.* 105 (1983) 1401; (b) G. Jeske, H. Lauke, H. Mauermann, H. Schumann, T.J. Marks, *J. Am. Chem. Soc.* 107 (1985) 8111; (c) V.P. Conticello, L. Brard, M.A. Giardello, Y. Tsuji, M. Sabat, C.L. Stern, T.J. Marks, *J. Am. Chem. Soc.* 114 (1992) 2761. [3] M. Giardello, V.P. Conticello, L. Brard, M.R. Gagne, T.J. Marks, *J. Am. Chem. Soc.* 114 (1994) 10241. [4] (a) D.G.H. Ballard, A. Courtis, J. Holton, J. McMeeking, R. Pearce, *J. Chem. Soc. Chem. Commun.* (1978) 994.; (b) P.L. Watson, *J. Am. Chem. Soc.* 104 (1982) 337; (c) E.E. Bunel, B.J. Burger, J.E. Bercaw, *J. Am. Chem. Soc.* 110 (1988) 976; (d) E.B. Coughlin, J.E. Bercaw, *J. Am. Chem. Soc.* 114 (1992) 7606; (e) S. Hajela, J.E. Bercaw, *Organometallics* 13 (1994) 1147; (f) G. Jeske, H. Lauke, H. Mauermann, P.N. Swepston, H. Schumann, T.J. Marks, *J. Am. Chem. Soc.* 107 (1985) 8091; (g) M.A. Giardello, Y. Yamamoto, L. Brard, T.J. Marks, *J. Am. Chem. Soc.* 117 (1995) 3276. [5] (a) M.R. Gagne, T.J. Marks, *J. Am. Chem. Soc.* 111 (1989) 4108; (b) M.R. Gagne, C.L. Stern, T.J. Marks, *J. Am. Chem. Soc.* 114 (1992) 275; (c) Y. Li, T.J. Marks, *J. Am. Chem. Soc.* 120 (1998) 1757; (d) V.M. Arredondo, F.E. McDonald, T.J. Marks, *J. Am. Chem. Soc.* 120 (1998) 4871. [6] (a) S.P. Nolan, M. Porchia, T.J. Marks, *Organometallics* 10 (1991) 1450; (b) T. Sakakura, H.J. Lautenschlager, M. Tanaka, *J. Chem. Soc. Chem. Commun.* (1991) 40.; (c) G.A. Molander, P.J. Nichols, *J. Am. Chem. Soc.* 117 (1995) 4414; (d) G.A. Molander, W.A. Retsch, *Organometallics* 14 (1995) 4570; (e) P.F. Fu, L. Brard, Y. Li, T.J. Marks, *J. Am. Chem. Soc.* 117 (1995) 7157. [7] (a) K.N. Harrison, T.J. Marks, *J. Am. Chem. Soc.* 114 (1992) 9220; (b) E.A. Bijpost, R. Duchateau, J.H. Teuben, *Mol. Catal.* 95 (1995) 121. [8] (a) Y.J. Luo, Y.M. Yao, Q. Shen, J. Sun, L.H. Weng, *J. Organomet. Chem.* 662 (2002) 144; (b) S. Bambirra, A. Meetsma, B. Hessen, J.H. Teuben, *Organometallics* 20 (2001) 782; (c) R. Duchateau, C.T. van Wee, A. Meetsma, P.T. van Duijnen, J.H. Teuben, *Organometallics* 15 (1996) 2279; (d) R. Duchateau, A. Meetsma, J.H. Teuben, *Organometallics* 15 (1996) 1656; (e) R. Duchateau, C.T. van Wee, J.H. Teuben, *Organometallics* 15 (1996) 2291; (f) F. Edelmann, *Coord. Chem. Rev.* 137 (1994) 403; (g) J. Barker, M. Kilner, *Coord. Chem. Rev.* 133 (1994) 219. [9] (a) P.J. Bailey, S. Pace, *Coord. Chem. Rev.* 214 (2001) 91; (b) Y.L. Zhou, G.P.A. Yap, D.S. Richeson, *Organometallics* 17 (1998) 4387; (c) Z.P. Lu, G.P.A. Yap, D.S. Richeson, *Organometallics* 20 (2001) 706; (d) G.R. Giesbrecht, G.D. Whitener, J. Arnold, *J. Chem. Soc. Dalton Trans.* (2001) 923.; (e) Y.J. Luo, Y.M. Yao, Q. Shen, K.B. Yu, L.H. Weng, *Eur. J. Inorg. Chem.* (2003) 318.; (f) Y.J. Luo, Y.M. Yao, Q. Shen, *Macromolecules* 35 (2002) 8670.

- [10] L. Bourget-Merle, M.F. Lappert, J.R. Severn, *Chem. Rev.* 102 (2002) 3031.
- [11] P.G. Hayes, W.E. Piers, R. McDonald, *J. Am. Chem. Soc.* 124 (2002) 2132.
- [12] L.S. Mao, Q. Shen, J. Sun, *J. Organomet. Chem.* 566 (1998) 9.
- [13] K.H. Haan den, J.L. de Boer, J.H. Teuben, *Organometallics* 5 (1986) 1726.
- [14] W.J. Evans, R.A. Keyer, J.W. Ziller, *Organometallics* 12 (1993) 2618.
- [15] M.Q. Xue, Q. Shen, Z.J. Zhang, L.S. Mao, *J. Rare Earths* 17 (1999) 495.
- [16] M.Q. Xue, L.S. Mao, Q. Shen, J.L. Ma, *Chin. J. Appl. Chem.* 16 (1999) 102.
- [17] M. Yamashita, Y. Takemoto, E. Ihara, H. Yasuda, *Macromolecules* 29 (1996) 1798.
- [18] Y.J. Luo, Q. Shen, Unpublished data.
- [19] L.S. Mao, Q. Shen, *J. Polym. Sci. A* 36 (1998) 1593.
- [20] C.T. Qian, W.L. Nie, J. Sun, *Organometallics* 19 (2000) 4134.
- [21] R.C. Ferugusan, D.W. Overall, *Polym. Prepr. (Am. Chem. Soc. Div. Polym. Chem.)* 26 (1985) 182.
- [22] M.D. Taylor, C.P. Carter, *J. Inorg. Nucl. Chem.* 24 (1962) 387.